Journal of Applied Electrochemistry **31**: 961–967, 2001.

Electrochemical and surface properties of aluminium in citric acid solutions

M. ŠERUGA* and D. HASENAY
Department of Physical Chemistry and Electrochemistry, Faculty of Food Technology, University of Osijek, F. Kuhača 18, HR-31000 Osijek, Croatia
*(*author for correspondence, fax: +385 31 207 115, e-mail: serugam@ptfos.hr)*

Received 21 May 2000; accepted in revised form 20 February 2001

Key words: aluminium, citric acid, corrosion, oxide film, surface processes

Abstract

The electrochemical and surface properties of aluminium in 0.05 M citric acid solutions of pH 2–8 were studied by means of open circuit potential (OCP), potentiodynamic polarization and potentiostatic current–time transient measurements. The OCP reached a steady-state value very slowly, probably due to the slow rate of detachment of surface complexes into the solution. Aluminium exhibits passive behaviour in citric acid solutions of pH 4–8. Tafel slopes b_c were characteristic for hydrogen evolution on aluminium covered by an oxide film. The corrosion kinetic parameters E_{corr}, i_{corr} and b_a suggest that surface processes are involved in the dissolution kinetics, especially in the pH range 3–6. Current–time transient measurements confirm that, in citric acid solutions of pH 3–6, the dissolution is controlled by surface processes, that is, by the rate of detachment of surface complexes, while in solutions of pH 2, 7 and 8 dissolution is under mass-transport control. The addition of fluoride ions to citric acid changes the controlling steps of the dissolution process. Citrate and fluoride ions compete for adsorption sites at the oxide surface, and adsorption of these ions is a competitive and reversible adsorption.

1. Introduction

Aluminium and its alloys has attracted many investigations of its electrochemical and other properties in different electrolytes: salts, alkalis and acids [1–7], due to its widespread industrial applications. In some applications (e.g., in the food industry) aluminium is in contact with citric acid or citrate ions from the foods. However, no systematic study of the electrochemical and/or surface properties of aluminium in citric acid or citrate solutions has been found in the literature. A few papers deal with some aspects of behaviour of aluminium or aluminium alloys, mainly corrosion, in contact with citric acid or citrate ions [8–12]. The corrosion rate of aluminium or aluminium alloys in acidic and neutral solutions of citric acid or citrate of pH range 3–7 is very small and does not significantly change within this pH range, but increases greatly in solutions of higher pH. It was also reported that citrate ions from the bulk solution may be adsorbed at the oxide-solution interface forming surface complexes, thus markedly influencing the dissolution kinetics of aluminium [12].

The aim of the present work was to study the electrochemical and surface properties of a high purity (99.999%) aluminium electrode in 0.05 M citric acid solutions with pH in the range 2–8. The techniques used are open circuit potential (OCP) measurements, potentiodynamic polarization and potentiostatic current–time transients. The measurements are performed using stationary and rotating disc electrodes. The kinetics and mechanism of the electrochemical processes on aluminium covered by a thin oxide film, at different pHs in citric acid solutions, are investigated.

2. Experimental details

The aluminium sample selected for the study was of high purity (99.999%, Al5N). Prior to each electrochemical experiment, the electrode surface was mechanically polished with emery paper (from 400 to 1200 grade) and then polished up to a mirror finish using a water suspension of 0.3 μm-Al_2O_3 powder. The electrode was then thoroughly rinsed with doubly distilled water. In all measurements the counter electrode was a platinum gauze and the reference electrode was a saturated calomel electrode (SCE), connected to a Luggin capillary filled with the working solution. All measured potentials are referred to the SCE.

The measurements were carried out in a standard water-jacketed electrochemical cell (Metrohm), connected to a constant temperature circulator. The measurements were performed at 25 °C.

The measurements were performed in 0.05 M citric acid solutions of different pHs (2, 3, 4, 5, 6, 7 and 8). The pH value of the initial stock solution of 0.05 M citric

acid (pH 2.3) was adjusted to the appropriate pH value by the addition of small amounts of concentrated NaOH (for solutions of pH 3 to 8) or very small amounts of concentrated $HClO_4$ (for a solution of pH 2). All solutions were prepared from analytical grade chemicals and doubly distilled water. The solutions used in electrochemical measurements were deaerated by pure argon before and during the measurements.

Electrochemical measurements were performed using an EG&G PARC model 273A potentiostat/galvanostat, remotely controlled by the computer with appropriate software. Measurements with a rotating disc electrode were made using an EG&G PARC model 636 electrode rotator system. For the OCP against time measurements, the microprocessor mV-meter Iskra MA 5740 connected with printer Iskra MA 9154 was used.

3. Results and discussion

3.1. *OCP measurements*

The aluminium electrode was immersed in the deaerated citric acid solution and the variation of the OCP with time was recorded until a steady-state value was reached. The observed OCP–time behaviour of the aluminium electrode was generally similar in citric acid solutions of pH 2, 3, 4, 5, 6 and 7, but was different for pH 8. In Figure 1 examples of OCP–time curves, which illustrate both types of behaviour are shown.

The results for citric acid solutions of pH range 2 to 7 generally show the following: (i) the OCP values changed continuously for a long period (more rapidly during the first several hours) and reached a steady value very slowly, and (ii) there were considerable changes in the OCP between the initial and steady-state values (reaching several hundreds millivolts). Both these results indicate significant changes of the surface oxide film during the immersion time. Similar results were reported for aluminium in acetate solutions and in mixtures of acetate and oxalate [2, 3], for Al-7075 alloy in oxalate solutions [13], and for Al-3003 and Al-5052 alloys in citrate and acetate buffer solutions [9]. It was suggested [3, 13] that specific adsorption of oxalate ions and the formation of strong surface complexes play an important role in Al and Al-alloy corrosion in oxalate. The detachment of surface Al-oxalate complexes was proposed as the rate determining step [3]. Similar results for dissolution kinetics of an oxide covered aluminium electrode were observed in solutions containing other strong complexing organic ligands [12]. The detachment of Al-surface complexes into the solution is usually a very slow process [12, 14–16]. Also, there is, during immersion, an ongoing surface oxide transformation process, that is, oxide film growth and ageing of the aluminium oxide film. Therefore, in solutions of citric acid in the pH range 2–7, the very slow reaching of steady-state OCP of aluminium electrode means that besides the electrochemical process, surface coordination processes also play an important role.

The shape of the potential-time curves observed in the solution of citric acid pH 8, is quite different from those recorded in solutions of pH 2 to 7. The initial rapid negative shift of potential in a relatively short time and reaching of steady-state value of potential after about 20 h of immersion may indicate relatively strong dissolution of preimmersion oxide and passive film formed at OCP, and/or the metal dissolution at sites with structural flaws in the oxide film.

3.2. *Polarization measurements*

3.2.1. *Polarization measurements in wide potential region*

After the OCP measurements the potentiodynamic polarization of aluminium electrode was performed from the region of hydrogen evolution (−1.5 V) to the anodic potential limit of 1.5 V, with a scan rate of 1 mV s^{-1}. It was shown that the profiles of polarization curves depend on the immersion time.

The effect of the immersion time at the OCP on the shape of polarization curves in citric acid solution of pH 6 is shown in Figure 2. These curves represent behaviour observed in solutions of citric acid in the pH range 4–7. The shape of the curves confirms the valve

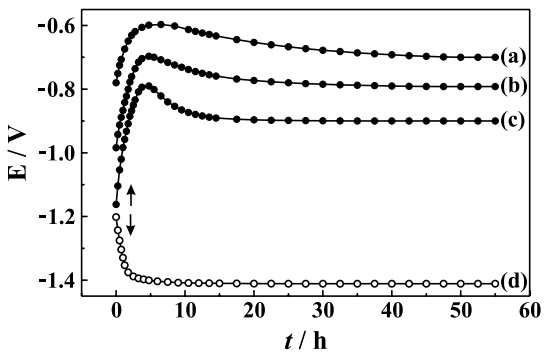

Fig. 1. Open circuit potential (OCP) vs time measurements for aluminium electrode in 0.05 M citric acid solutions of different pH: (a) 2, (b) 4, (c) 6 and (d) 8.

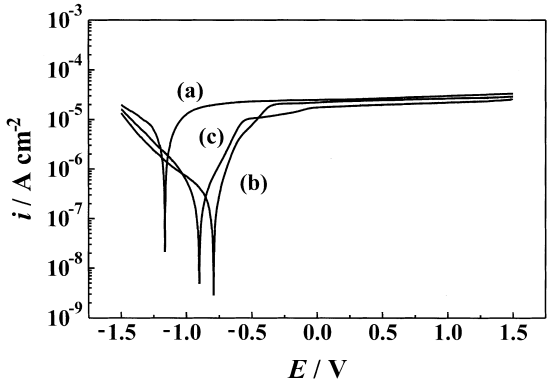

Fig. 2. Potentiodynamic polarization curves for aluminium electrode obtained after different immersion times at the OCP in 0.05 M citric acid solution of pH 6. Immersion time: (a) 0.5, (b) 5 and (c) 50 h. Scan rate, $v = 1$ mV s^{-1}.

behaviour of aluminium, that is, the rectification mechanism of electron transfer reaction (blocked anodic, but not cathodic electron transfer). There was a small and practically constant anodic current between 0.0 V and 1.5 V, indicating the passive behaviour of the aluminium electrode (i.e., existence of an oxide layer on the electrode surface). The film formed on aluminium during anodic polarization in citric acid or citrate solutions is a thin barrier-type oxide film [17, 18].

An analysis of the polarization plots indicates that the passivation current decreases with increase in immersion time. As the current established during the oxide film formation process is a measure of the protective capability of the oxide, its decrease with increase of the immersion time is due to the thickening of the oxide film layer, and/or the ordering of the oxide film structure. It was thus observed that increase of the immersion time was favourable to the formation of a more resistive film and leads to more stable current–voltage shapes.

The effect of pH on the shape of potentiodynamic polarization curves of aluminium is shown in Figure 3. Three different types of curve are observed. In a citric acid solution of pH 6 the aluminium electrode shows typical passive behaviour, due to the formation of a thin barrier-type passive film. Similar behaviour, as in a solution of pH 6, was also observed in citric acid solutions of pH 4, 5 and 7.

In a solution of citric acid pH 8, the curve shape indicates that the relatively strong dissolution of oxide film coexists with the passivation process (strong oscillation of current during the anodic polarization). In a solution of citric acid pH 2 there was no additional passive film formation during the anodic polarization. Strong dissolution of the preimmersion oxide air-formed film and the film-destroying effect, probably due to the high concentration of H^+ ions, prevents formation of the passive film during anodization [19], and a breakdown of the passivity and/or strongly local metal dissolution occur. Very similar behaviour was also observed in citric acid of pH 3.

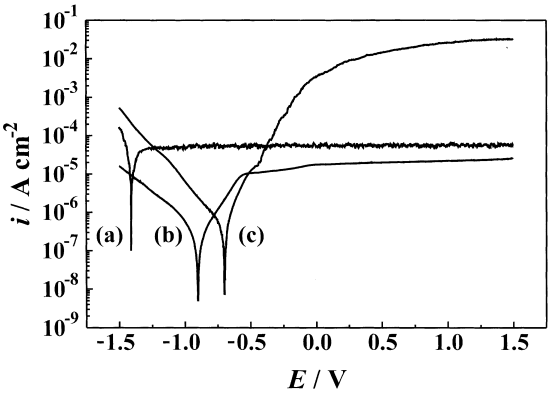

Fig. 3. Potentiodynamic polarization curves for aluminium electrode obtained after 50 h of immersion at the OCP in 0.05 M citric acid solutions of different pH values: (a) 8, (b) 6 and (c) 2. Scan rate, $v = 1$ mV s^{-1}.

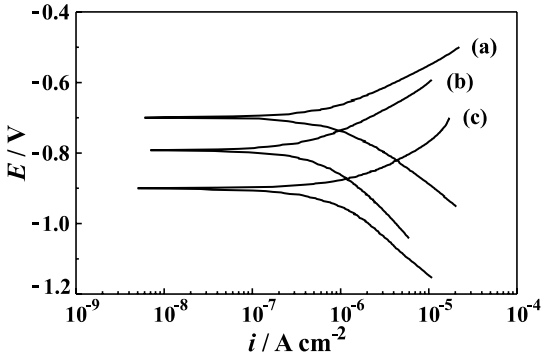

Fig. 4. Tafel plots for aluminium electrode obtained after 50 h of immersion at the OCP in 0.05 M citric acid solutions of different pH values: (a) 2, (b) 4 and (c) pH 6. Scan rate, $v = 1$ mV s^{-1}.

3.2.2. *Polarization measurements in Tafel region*

After the steady-state OCP value was reached (Figure 1), the aluminium electrode was polarized by the potentiodynamic method with a scan rate of 1 mV s^{-1}, beginning the scan at −250 mV vs E_{corr} and scanning continuously to +200 mV vs E_{corr}, that is, in the so-called Tafel region.

All the potentiodynamic polarization curves have similar shapes, and examples are shown in Figure 4. The corrosion kinetic parameters E_{corr}, i_{corr}, b_c and b_a, determined from polarization curves in the Tafel region by the use of PARCalc^{TM} numerical analysis program [20], are summarized in Table 1.

The values of corrosion potential (E_{corr}) of aluminium electrodes shift negatively with increase in pH (Figure 5). On the E_{corr} vs pH curve, three different regions are observed. In the pH range 2–3, there is a very small change in E_{corr}. Because in the pH range 2–3 the concentration of H^+ ions is sufficiently high and oxygen is eliminated from solutions, the dissolution of aluminium in this pH region is under the control of electrochemical processes. This means that the main cathodic process is a reduction of H^+ ions and the evolution of hydrogen, and the main anodic process is the dissolution of aluminium in the form of Al^{3+} aqueous complexes.

Table 1. Corrosion kinetic parameters E_{corr}, i_{corr}, b_c and b_a for aluminium electrode in 0.05 M citric acid solutions of different pH values, determined from the Tafel plots

pH	E_{corr} /V	i_{corr} /μA cm^{-2}	b_c /mV	b_a /mV
2	−0.700	0.91	−205	113
3	−0.720	0.73	−235	115
4	−0.792	0.57	−263	127
5	−0.849	0.45	−256	140
6	−0.900	0.89	−214	144
7	−1.091	2.01	−165	290
8	−1.411	27.69	−140	343

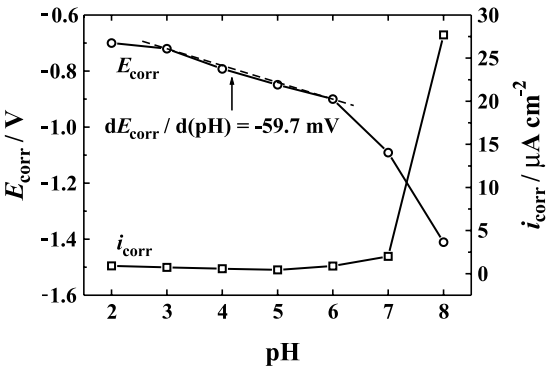

Fig. 5. Dependence of corrosion potentials (E_{corr}) and corrosion current densities (i_{corr}) of aluminium electrode, determined from Tafel plots, on the pH values of 0.05 M citric acid solutions.

E_{corr} against pH behaviour in the pH region 6–8 was characterized by a strong negative shift of E_{corr} with increase in pH. At the same time, the corrosion current density (i_{corr}) increased significantly with increase in pH (Table 1, Figure 5), especially in solution of pH 8. Thus the dissolution of aluminium increases significantly from pH 6 to 8, especially from pH 7 to 8. Such behaviour is in agreement with the fact that aluminium dissolves relatively strongly at these pH values as aluminate AlO_2^- or $Al(OH)_4^-$ ion [1]. It seems that the electrochemical corrosion mechanism (evolution of hydrogen, dissolution of aluminium as aluminate ion) proceedes in this pH range, especially at pH 8.

Indicative E_{corr} against pH behaviour was observed in solutions of citric acid in the pH range 3–6, where E_{corr} changes linearly with pH, and the slope of the E_{corr} against pH curve was –59.7 mV per unit pH. This behaviour can be explained as follows.

In aqueous solutions Al-oxide surface is significantly hydrated. The hydration of aluminium-oxygen bonds on the oxide film leads to the formation of surface –OH groups. Subsequent amphoteric dissociation of –OH groups leads to the development of a charge on the oxide surface [21, 22]. Therefore, an acid–base equilibrium is established on the surface with a characteristic pH of zero charge (pH_{pzc}), which controls the surface charge and the surface processes (e.g., adsorption) on an oxide covered Al-electrode. Very different data have been reported concerning the pH_{pzc} for different aluminium oxides and hydroxides and metallic aluminium (most of the reported values lie between pH 7–9) [23]. Therefore, at pH lower than 7–9 the aluminium surface probably has a net positive charge (due to adsorption of H^+ ions $-OH_2^+$ surface sites are formed), and anions are attracted to the surface and may be adsorbed. This adsorption may be electrostatic and/or chemical in nature (surface complexation and/or ligand exchange reactions [14–16]). Interaction between surface and anions, that is, surface reactions, may also occur on neutral surface sites, that is, at –OH groups (e.g., chemisorption and/or ligand exchange reactions [14–16]).

In citric acid solution the possible surface complexing ligands are H_2Cit^-, $HCit^{2-}$ and Cit^{3-} species. The amount of these ligands in solution depends on the pH (e.g., in solution of citric acid of pH 6 prevailed $HCit^{2-}$ species). Therefore, on an aluminium oxide surface in contact with citric acid solutions, a number of different surface coordination reactions occur, which result in a number of different aluminium-citrate and/or aluminium-hydroxo-citrate surface species. The nature and the structure of these surface complexes is practically unknown, although some authors [24, 25] have reported a possible two six-membered chelate ring structure of surface Al-citrate complexes. Also, some authors have confirmed by surface analysis techniques, for example, by Auger electron spectroscopy (AES) [26] and glow discharge optical emission spectroscopy (GDOES) [18], that citrate anions are adsorbed on the oxide surface and incorporated into the structure of the oxide film during the anodic oxidation of aluminium in citric acid and/or citrate solutions.

We can only speculate about the possible structure and composition of the surface complexes at the aluminium oxide/citric acid interface. However, the general principle of possible surface coordination reactions [12, 14–16], which occur at aluminium oxide surfaces in solutions of citric acid of pH range 3–6, can be illustrated by the possible surface reactions in solution of pH 6:

$$> Al\text{–}OH_2^+ + HCit^{2-} \rightleftharpoons > AlHCit^- + H_2O \qquad (1)$$

$$> Al\text{–}OH + HCit^{2-} \rightleftharpoons > AlHCit^- + OH^- \qquad (2)$$

Therefore, the observed characteristic E_{corr} against pH behaviour in the pH range 3–6 probably reflects an acid–base equilibrium established at aluminium oxide covered electrodes and the surface coordination processes. It seems that in solutions of citric acid of pH 3–6, the different surface coordination processes play an important role in the dissolution kinetics.

From the polarization curves, the kinetic parameters of the corrosion process mechanism, b_c and b_a, were examined (Table 1). The polarization experiments were performed in argon-deaerated solutions to eliminate the influence of oxygen electroreduction on the curves. Thus the cathodic process occurring at the Al-oxide/citrate solution interface was hydrogen evolution. Table 1. shows that the cathodic Tafel slopes (b_c) are much greater than that expected for H_2 evolution according to the Volmer–Tafel mechanism [27] (–118 mV (decade)$^{-1}$ at 298 K). Such anomalously large cathodic Tafel slopes are not unexpected for aluminium, and have previously been reported for H_2 evolution reaction on Al oxide-covered electrodes [2–5, 9, 28, 29]. The presence of the oxide film can markedly influence the surface reduction process, by affecting the energetics of the reaction at the double layer, or by imposing a barrier to charge transfer through the oxide film, or both.

The anodic Tafel slopes (b_a) are much greater than the expected 40 mV (decade)$^{-1}$ corresponding to the uniform anodic dissolution of aluminium via hydrated Al^{3+} ions. The observed b_a values (Table 1) are in agreement with the b_a values reported for an Al oxide-covered electrode [2–5], which clearly indicates the presence and growth of a passive oxide film. However, the b_a greater than those for the simple aluminium dissolution mechanism ($Al \rightarrow Al^{3+} + 3e^-$), can also be attributed to the participation of some side reactions (e.g., surface coordination reactions) in anodic oxide film growth.

The corrosion current densities (i_{corr}) are presented in Figure 5 and Table 1. As can be seen in Figure 5, the i_{corr} values are very small, except in citric acid of pH 8. In solutions of pH range 3–6 some kind of 'dissolution current plateau' is observed. This behaviour can be explained as follows. The dissolution (solubility) of aluminium, Al-hydroxide and various forms of Al oxide in water and noncomplexing solutions is very small, and the minimum solubility of the Al oxides and Al hydroxide is clearly expressed at pH 5 [1]. However, in aqueous complex-forming solutions (e.g., citrate, oxalate, salicylate) the minimum solubility is not so well expressed; a 'plateau of dissolution' is observed at some pH range [14, 30], and the dissolution is controlled by surface complexation reactions [12, 14–16]. It seems that dissolution of aluminium in citric acid in the pH range 3–6 also proceedes by the same mechanism.

3.3. *Measurements with rotating disc electrode*

Dissolution current density (i) against time (t) measurements for an aluminium rotating disc electrode on the potentiostatically controlled potential (E) in citric acid solutions of pH range 2–8 were performed. The potentials chosen for measurements were the E_{corr} values of each citric acid solution (Table 1). The electrode was polarized potentiostatically at a corresponding potential at $t = 0$ until the steady-state dissolution current density (i_{ss}) was reached.

All the current–time transients have similar shapes, an example is shown in Figure 6. The decrease of current density with time probably reflects a barrier oxide film formation and/or the ordering of the oxide film structure.

The current–time measurements were performed at different rotation rates of the Al-disc electrode (0–2500 rpm) in citric acid in the pH range 2–8. As can be seen in Figure 7, in the pH range 3–6, i_{ss} does not depend on the transport parameter (rotation rate of the disc), which is typical of a surface reaction controlled dissolution process. In citric acid of pH 2 and 7, and especially in solution of pH 8, i_{ss} increases linearly with rotation rate. This linear dependence is characteristic of a mass-transport controlled dissolution process [12].

To study the influence of other anions (e.g., fluoride ions) on the dissolution kinetics of aluminium in citric acid, an experiment with successive additions of fluoride

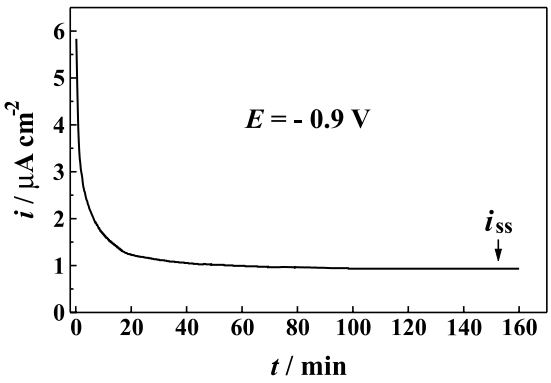

Fig. 6. Potentiostatic current–time transient for aluminium disc electrode recorded at constant electrode potential ($E = -0.9$ V) in 0.05 M citric acid solution of pH 6. Rotation rate 2000 rpm.

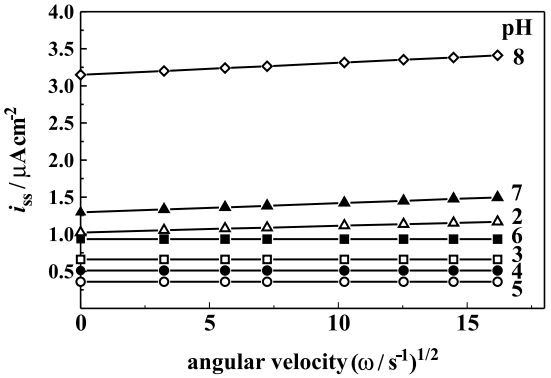

Fig. 7. Influence of angular velocity (ω) of the aluminium disc electrode on the steady-state dissolution current densities (i_{ss}), obtained from potentiostatic current–time transients recorded at constant electrode potentials (corresponded E_{corr} values) in 0.05 M citric acid solutions of different pH values.

in citric acid of pH 6 was performed (Figure 8). On addition of fluoride to the citric acid solution, the dissolution current density increased significantly. After the first fluoride addition the steady-state reached very slowly, but subsequent additions of fluoride caused

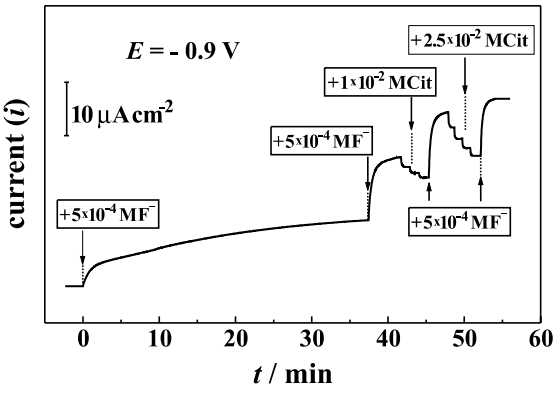

Fig. 8. Influence of successive additions of fluoride and citrate ions on the current–time transients, recorded at constant electrode potential ($E = -0.9$ V), for aluminium disc electrode in 0.05 M citric acid solution of pH 6. Rotation rate 2000 rpm.

abrupt increase in the dissolution current and the relaxation time was shorter. The steady-state dissolution current density was proportional to the fluoride bulk concentration.

The addition of citrate to the fluoride-contained solution decreased the dissolution current (Figure 8). This decrease was proportional to the concentration of added citrate ions. The steady-state was reached rapidly (relaxation time is very short). The concentration step experiments (Figure 8) were very reproducible and controlled by the mixing of solution (rotation rate of the disc).

These results can be interpreted in terms of competitive and reversible adsorption between fluoride and $HCit^{2-}$ ions (prevailed citrate species in solution of pH 6):

$$\begin{array}{ll} > AlHCit^{-} + xF^{-} \underset{\text{fast}}{\overset{\text{slow}}{\rightleftharpoons}} > AlF_x^{1-x} + HCit^{2-} & \\ k_{Cit} \downarrow \text{slow} & k_{F^-} \downarrow \text{fast} \\ AlHCit^{+}(aq) & AlF_x^{3-x}(aq) \end{array} \quad (3)$$

where k_{Cit} is much less than k_{F^-} [12, 14–16].

The addition of fluoride to citric acid changes the controlling steps of the dissolution process. As can be seen in Figure 9, in solution of 'pure' citric acid of pH 6 dissolution is controlled by a surface processes. In fluoride-contained citric acid solution of pH 6 the dissolution is under mixed control, that is, the dissolution process is controlled by mass transport of fluoride ions to the oxide/solution interface and by the surface processes.

4. Conclusions

The electrochemical and surface properties of aluminium in 0.05 M citric acid solutions of pH 2–8 were studied by means of open circuit potential (OCP), potentiodynamic polarization and potentiostatically controlled current–time transient measurements.

The results show that the OCP reached a steady-state value very slowly, probably due to the slow rate of detachment of surface complexes into the solution. Potentiodynamic polarization measurements show that aluminium exhibits passive behaviour in citric acid solutions of pH 4–8, due to the formation of a thin barrier-type of passive oxide film. Polarization curves give cathodic Tafel slopes (b_c) characteristic for hydrogen evolution on oxide-film covered aluminium. The values of corrosion kinetic parameters E_{corr}, i_{corr} and anodic Tafel slopes (b_a), especially in the solution of pH 3–6, suggest that surface processes are probably involved in the dissolution kinetics of aluminium. Measurements with a rotating disc electrode show that in citric acid solutions of pH 2, 7, and 8 the dissolution process is controlled by mass transport, while in solutions of pH 3–6, the dissolution of aluminium is controlled by surface reactions (adsorption, surface complexation). Adsorption of electrolyte anions on the hydrated aluminium oxide covered electrode is competitive and reversible. There is a competition between the citrate and fluoride ions from the bulk solution for adsorption sites at the oxide surface, and the extent of adsorption of these anions depends on their specific affinity for the surface aluminium atoms in the oxide film and on the concentration of free anions in the bulk solution.

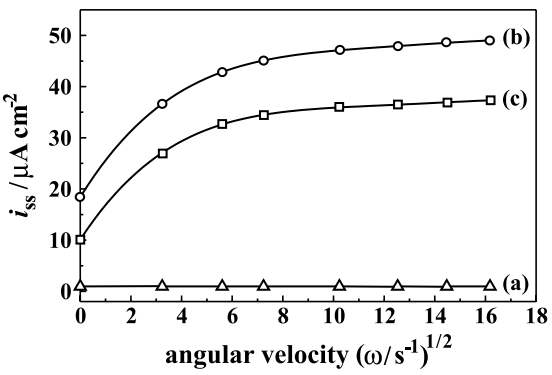

Fig. 9. Influence of angular velocity (ω) of the aluminium disc electrode on the steady-state dissolution current densities (i_{ss}), obtained from potentiostatic current–time transients recorded at constant electrode potential ($E = -0.9$ V) in different citric acid + fluoride solutions of pH 6: (a) 0.05 M citric acid, (b) 0.05 M citric acid + 2×10^{-3} M fluoride, (c) 0.25 M citric acid + 2×10^{-3} M fluoride.

References

1. E. Deltombe, C. Vanleugenhaghe and M. Pourbaix, Aluminium, *in* M. Pourbaix (Ed.), 'Atlas of Electrochemical Equilibria in Aqueous Solutions' (Pergamon Press-Cebelcor, Oxford and Brussels, 1966), pp. 168–176.
2. T. Hurlen, H. Lian, O.S. Ødegard and T. Valand, *Electrochim. Acta* **29** (1984) 579.
3. W. Wilhelmsen and A.P. Grande, *Electrochim. Acta* **33** (1988) 927.
4. M. Metikoš-Huković, R. Babić, Z. Grubač and S. Brinić, *J. Appl. Electrochem.* **24** (1994) 325.
5. M. Metikoš-Huković, R. Babić, Z. Grubač and S. Brinić, *J. Appl. Electrochem.* **24** (1994) 772.
6. H.J.W. Lenderink, M.v.d. Linden and J.H.W. de Wit, *Electrochim. Acta* **38** (1993) 1989.
7. S.-M. Moon, S.-I. Pyun, *Electrochim. Acta* **44** (1999) 2445.
8. K.F. Lorking and J.E.O. Mayne, *J. Appl. Chem.* **11** (1961) 170.
9. S. Evans and E.L. Koehler, *J. Electrochem. Soc.* **108** (1961) 509.
10. M.S. Abdel-Aal, M.T. Makhlouf and A.A. Hermas, *J. Electrochem. Soc. India* **42** (1993) 165.
11. M. Katoh, *Corros. Sci.* **8** (1968) 423.
12. V. Žutić and W. Stumm, *Geochim. Cosmochim. Acta* **48** (1984) 1493.
13. L. Kobotiatis, N. Pebere and P.G. Koutsoukos, *Corros. Sci.* **41** (1999) 941.
14. G. Furrer and W. Stumm, *Chimia* **37** (1983) 338.
15. G. Furrer and W. Stumm, *Geochim. Cosmochim. Acta* **50** (1986) 1847.
16. W. Stumm, G. Furrer and B. Kunz, *Croat. Chem. Acta* **56** (1983) 593.
17. G.A. Hutchins and C.T. Chen, *J. Electrochem. Soc.* **133** (1986) 1332.

18. K. Shimizu, G.M. Brown, H. Habazaki, K. Kobayashi, P. Skeldon, G.E. Thompson and G.C. Wood, *Electrochim. Acta* **44** (1999) 2297.
19. P.L. Cabot, F.A. Centellas, J.A. Garrido and E. Perez, *J. Appl. Electrochem.* **17** (1987) 104.
20. Model 352/252 Corrosion Analysis Software 2.01 Instruction Manual, EG&G PAR, New Jersey (1992).
21. M.J. Dignam, Mechanisms of ionic transport through oxide films, *in* J.W. Diggle (Ed.), 'Oxides and Oxide Films', Vol. 1 (Marcel Dekker, New York, 1972), pp. 168–169.
22. S.M. Ahmed, Electrical double layer at metal oxide–solution interfaces, *in* J.W. Diggle (Ed.), Vol. 1, *op. cit.* [21], pp. 412–443.
23. G.A. Parks, *Chem. Rev.* **65** (1965) 177.
24. G. Sposito (Ed.), 'The Environmental Chemistry of Aluminum' (Lewis Publishers, Boca Raton, 1996), pp. 173–174 and 303–305.
25. P.C. Hidber, T.J. Graule and L.J. Gauckler, *J. Am. Ceram. Soc.* **79** (1996) 1857.
26. V.F. Surganov, *Russ. J. Electrochem.* **30** (1994) 742.
27. J.O'M. Bockris and A.K.N. Reddy, 'Modern Electrochemistry', Vol. 2 (Plenum Press, New York, 1974), pp. 862–910.
28. A.K. Vijh, *J. Phys. Chem.* **73** (1969) 506.
29. A.K. Vijh, Anodic oxide films: Influence of solid-state properties on electrochemical behaviour, *in* J.W. Diggle (Ed.), Vol. 2 (1973), *op. cit.* [21], pp. 70–78.
30. L.-O. Öhman, *Inorg. Chem.* **27** (1988) 2565.